HHS Public Access

Author manuscript

Cell Rep. Author manuscript; available in PMC 2017 January 27.

Published in final edited form as:

Cell Rep. 2014 December 24; 9(6): 2034–2042. doi:10.1016/j.celrep.2014.11.040.

Conversion of Fibroblasts to Neural Cells by p53 Depletion

Di Zhou[1,5], **Zhen Zhang**[2,5], **Li-Ming He**[2,5], **Juan Du**[1,5], **Fan Zhang**[1], **Chong-Kui Sun**[1], **Yu Zhou**[1], **Xiao-Wei Wang**[1], **Ge Lin**[3], **Ke-Ming Song**[4], **Ling-Gang Wu**[2,*], and **Qin Yang**[1,*]

[1]Cancer Biology Division, Washington University School of Medicine, Saint Louis, MO 63108, USA

[2]Synaptic Transmission Section, NINDS/NIH, Bethesda, MD 20892, USA

[3]Institute of Reproductive and Stem Cell Engineering, Central South University, Changsha 410078, China

[4]Research Biotechnology Business Unit, Sigma-Aldrich Corporation, St. Louis, MO 63103, USA

SUMMARY

Conversion from fibroblasts to neurons has recently been successfully induced. However, the underlying mechanisms are poorly understood. Here, we find that depletion of p53 alone converts fibroblasts into all three major neural lineages. The induced neuronal cells express multiple neuron-specific proteins and generate action potentials and transmitter-receptor-mediated currents. Surprisingly, depletion does not affect the well-known tumorigenic p53 target, p21. Instead, knockdown of p53 upregulates neurogenic transcription factors, which in turn boosts fibroblast-neuron conversion. p53 binds the promoter of the neurogenic transcription factor Neurod2 and regulates its expression during fibroblast-neuron conversion. Furthermore, our method provides a high efficiency of conversion in late-passage fibroblasts. Genome-wide transcriptional analysis shows that the p53-deficiency-induced neurons exhibit an expression profile different from parental fibroblasts and similar to control-induced neurons. The results may help to understand and improve neural conversion mechanisms to develop robust neuron-replacement therapy strategies.

Graphical abstract

*Correspondence: wul@ninds.nih.gov (L.-G.W.), qyang@wustl.edu (Q.Y.).

[5]Co-first author

ACCESSION NUMBERS

Data have been deposited in NCBI Gene Expression Omnibus and are accessible and are available under accession number GSE43175.

SUPPLEMENTAL INFORMATION

Supplemental Information includes Supplemental Experimental Procedures and four figures and can be found with this article online at http://dx.doi.org/10.1016/j.celrep.2014.11.040.

AUTHOR CONTRIBUTIONS

Q.Y. generated the hypotheses, designed experiments, and analyzed data. D.Z., Z.Z., L.-M.H., J.D., F.Z., Y.Z., C.-K.S., and G.L. performed experiments and generated data. L.-G.W., X.-W.W., and K.-M.S. designed experiments and analyzed data. Q.Y., D.Z., Z.Z., and L.-G.W. wrote the manuscript.

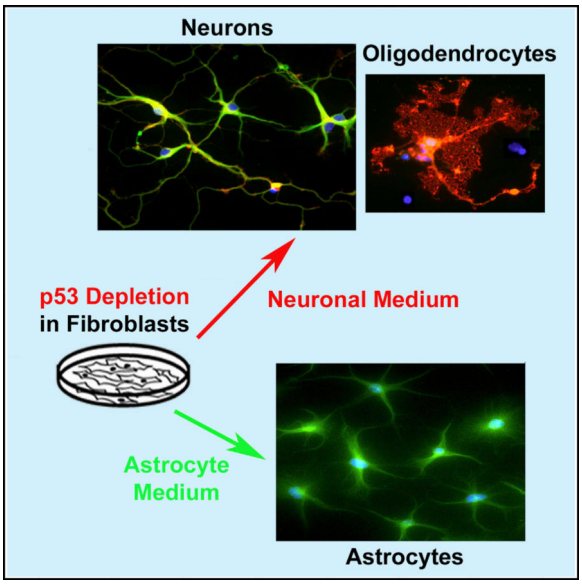

INTRODUCTION

Differentiated somatic cells have been reprogrammed to a pluripotent state by forced expression of a set of transcription factors (Takahashi et al., 2007), indicating that terminally differentiated cells can be induced to undergo cell fate change. Recent studies further demonstrated that direct conversion from fibroblast to neuron, a potential cell replacement therapy for neurological disorders, can be induced by a set of transcription factors without passing through a pluripotent state (Caiazzo et al., 2011; Vierbuchen et al., 2010; Pfisterer et al., 2011; Pang et al., 2011; Yoo et al., 2011; Ambasudhan et al., 2011). However, the mechanism underlying this conversion process remains largely unclear. As a result, a variety of combinations of transcription factors have been tried but generally with low percentages and very slow time course of conversion.

The p53 tumor suppressor reduces cancer initiation by inducing apoptosis, cell cycle, and senescence. For functions of p53 in the neural fate, it potently limits the growth of immature and mature neurons in response to a variety of stress signals. Recent studies show new roles of p53 in a wide range of processes, including neural precursor cell self-renewal, differentiation, and neuron fate decisions (Lanni et al., 2012; Hede et al., 2011; Mendrysa et al., 2011). Furthermore, p53 has been shown to inhibit reprogramming of fibroblasts to induced pluripotent stem cells (iPSCs) (Hong et al., 2009; Utikal et al., 2009; Kawamura et al., 2009), which raised a possibility that p53 might suppress fibroblast conversion to neurons. Here, we investigated whether p53 controls conversion of fibroblasts to neural cells. We found that depletion of *p53* alone could convert fibroblasts into astrocytes, oligodendrocytes, and functional neurons. Depletion of *p53* mediated this conversion by upregulating a set of neurogenic transcription factors.

RESULTS

Knockout of p53 Converts Fibroblasts into Neurons, Astrocytes, and Oligodendrocytes

We tested the possibility whether p53 might suppress fibroblast conversion to neurons by establishing a *p53*$^{-/-}$ cell line using zinc finger nuclease (ZFN) technology to knock out *p53* in normal human primary fibroblasts (IMR90). The *p53*-specific ZFNs are fusion proteins including the engineered zinc finger proteins that specifically bind to exon 3 of p53 genomic DNA and the nonspecific nuclease domain of restriction enzyme FokI that generates double-strand DNA cleavage. The repair of genomic DNA through the cellular process of nonhomologous end joining resulted in deletion of exon 3, creating a functional knockout of *p53*. *p53*$^{-/-}$ monoclonal lines were verified by quantitative PCR (qPCR), Southern and northern blot, and genomic DNA sequence (Figures S1A–S1D). The knockout was further evident in p53$^{-/-}$ cells, because p53 protein expression and p21, a p53 downstream target protein, were not detected (Figure 1A). Radiation-induced p21 was decreased, indicating that the p53 DNA damage pathway was disrupted.

To determine whether *p53* converts fibroblasts to three main neural lineages, astrocytes, neurons, and oligodendrocytes, we cultured *p53*$^{-/-}$ and *p53*$^{+/+}$ IMR90 fibroblasts in an astrocyte medium for astrocyte induction and a defined neuronal medium for neuron and oligodendrocyte induction (Figure 1B). In astrocyte medium, most *p53*$^{-/-}$ cells showed astrocyte morphology and were uniformly stained for glial fibrillary acidic protein (GFAP) and S100B (Figures 1C and 1D), whereas *p53*$^{+/+}$ cells kept fibroblast morphology with negative GFAP staining (Figures S1E and S1F). In neuronal medium, a low percentage (3%–5%) of induced cells showed oligodendrocyte markers O4- and MBP-positive staining with characteristic oligodendrocyte morphology (Figures 1C and 1D). In only 3 days in neuronal medium, we observed bipolar neuron-like cells. In 7 days, cells with more-mature neuronal morphology that expressed both Tuj1 (a neuronal marker) and MAP2 (a marker of postmitotic neurons) were present. In 3 or 4 weeks, 70%–85% of fibroblasts were converted to induced neuron cells (iNCs) (Figures 1C–1E). In contrast, after 4 weeks in neuronal medium, *p53*$^{+/+}$ cells kept fibroblast morphology with negative staining of O4 and MAP2 (Figures S1E and S1F). These results suggest that p53 deficiency led to direct conversion of human fibroblasts to neurons. To confirm conversion of fibroblasts to neurons by p53 deficiency, we used isogenic wild-type (*p53*$^{+/+}$) and knockout of *p53* (*p53*$^{-/-}$) mouse embryonic fibroblasts (MEFs) in the same induced media for neuronal cell induction. Consistent with the human IMR90 cells, 40%–50% of *p53*$^{-/-}$ MEFs were converted to iNCs 3 weeks after induction (Figures S1G and S1H), whereas *p53*$^{+/+}$ MEFs still kept fibroblast morphology.

iNCs by Knockdown of p53 Are as Functional Neurons

Whereas permanent p53 deletion converts fibroblasts to neurons, it may also cause genomic instability that increases the risk of cancer cell induction (Laiho and Latonen, 2003; Hofseth et al., 2004). To relieve this risk, we determined whether p53 knockdown was sufficient to induce fibroblast conversion to neural cells. Lentiviral constructs expressing short hairpin RNA against p53 (shp53) were transfected to wild-type IMR90 cells (Figure S2A). Transfected cells were converted into neural cells with kinetics and conversion efficiency

similar to *p53* knockout and showed Tuj-1- and MAP2-positive staining for neurons, GFAP for astrocytes, and O4 for oligodendrocytes (Figures 2A, 2F, and S2B). In contrast, cells expressing scrambled short hairpin RNA (shRNA) kept fibroblast morphology with negative staining of MAP2, O4, and GFAP after 4 weeks induction (Figures 2F and S2B).

So far, we identified iNCs based on their morphology and positive staining of several neuronal markers. In the following, we further characterized the functional aspects of iNCs induced by shp53 from IMR90 cells. We found that iNCs induced by p53 knockdown showed synapsin-positive puncta that label the vesicles in the presynaptic nerve terminal (Figure 2B). iNCs were positive in the immunostaining of vesicular glutamate transporter 1 (vGluT1) (glutamatergic neuron marker; Figure 2C) and GABA (GABAergic neuron marker; Figure 2D), suggesting that iNCs could be either excitatory or inhibitory. Quantification of the number of GABAergic or glutamatergic cells showed that 41% of iNCs (410/1,000) are immunopositive for GABA (GABAergic) and 48% of iNCs (480/1,000) are immunopositive for vGluT1 (glutamatergic). In addition, about 58% of iNCs with positive immunostainings for TBR1 indicate that iNCs have the similar identities to forebrain neurons (Figure 2E). They were negative in the immunostaining of motor neuron marker HOXB9, dopaminergic neuron marker tyrosine hydroxylase, and peripherin (data not shown).

To determine whether iNCs generate action potentials and neurotransmitter-induced currents, the basic functions of neurons, we cultured shp53-transfected IMR90 cells (7 days after induction) with a monolayer culture of primary rat neurons, which might provide a better environment for maturation (Pang et al., 2011; Vierbuchen et al., 2010). iNCs were identified by GFP fluorescence (Figure S2C). Two to three weeks after the coculture, whole-cell voltage-clamp recordings at iNCs showed that 68% of iNCs exhibited inward fast-activating and inactivating sodium currents and outward potassium currents during a step or a ramp depolarization (Figures 2G and 2H; n = 25). Current-clamp recordings of these iNCs showed multiple- or single-action potentials during inward current injection (Figure 2I; 68%; n = 25). Exogenous application of L-glutamate or GABA to iNCs that fired action potentials induced inward currents (glutamate: Figure 2J, 69%, n = 30; GABA: Figure 2K, 76%, n = 25), indicating the presence of postsynaptic functional glutamate and GABA receptors (Thier et al., 2012). Even more importantly, spontaneous synaptic currents, miniature excitatory postsynaptic currents (EPSCs), and miniature inhibitory postsynaptic currents (IPSCs) were recorded (Figure 2L), suggesting that iNCs can form functional synapses. Furthermore, we examined that the iNCs receive synaptic input of the maturation of electrophysiological properties of these neurons over time in culture. Twenty percent of iNCs fired single-action potentials after 1 week induction; however, the majority of iNCs were still silent. Forty-four percent or 68% of induced neurons (iNs) fired multiple-action potentials after induced for 2 or 3 weeks, respectively, suggesting that iNCs become mature gradually. Positive staining of human nuclei (specific marker for human cells) in all GFP-labeled iNCs indicates that electrophysiological recordings are from iNCs (Figure 2M). These data indicate that iNCs are functional neurons.

To confirm the effect of p53 knockdown on conversion of iNCs, we expressed shp53 in other human cells. Both normal adult dermal and neonatal foreskin fibroblasts with expression of

shp53 were effectively converted to iNCs 3 weeks after induction (Figure S2D), whereas *p53* wild-type cells still kept fibroblast morphology. iNCs were positive in the immunostaining of Tuj-1, MAP2, Synapsin, and TBR1, similar to iNCs from IMR90 cells. To address whether p53 has a general effect on human somatic cells, we expressed shp53 in human epithelia cells. After induction 3 weeks in a modified induction medium, about 15% of epithelia cells were converted into neurons (Figure S2D). Thus, inactivation of p53 by shp53 is able to convert different somatic cells into neurons.

Role of the p53-p21 Pathway in iN Conversion

We had showed that p53 knockout or knockdown induced fibroblast conversion to neurons (Figures 1 and 2). The induction was specific to p53 depletion, because overexpression of wild-type p53 in IMR90 cells expressing shp53 essentially abolished fibroblast-neuron conversion throughout the 3 or 4 weeks of time we monitored (Figures 3A, S3A, and S3B). Furthermore, overexpression of a p53 mutant, R273H, in which Arg 273 in the DNA-binding domain was replaced with His (Goh et al., 2011; Yang et al., 2002, 2004), did not affect the induction time course.

p21 is one of the most-prominent targets of p53 involved in regulation of cell cycle (Abbas and Dutta, 2009; Laiho and Latonen, 2003) and iPSC reprogramming (Hong et al., 2009; Kawamura et al., 2009; Lanni et al., 2012). To determine whether p53 depletion induced fibroblast-neuron conversion by inhibiting the p53-p21-signaling pathway, we inhibited p21 by infecting IMR90 cells with lentiviral constructs expressing shRNAs against p21 (shp21) (Figure S3C). Under this condition, we did not observe neuronal morphology in shp21-expressing cells in 4 weeks after induction (Figures 3B and S3D). Furthermore, coexpression of shp21 or wild-type p21 with shp53 did not affect shp53-induced fibroblast-neuron conversion in IMR90 cells (Figure 3C). These data indicate that p21 is not involved in shp53-induced fibroblast-neuron conversion.

In Vivo Analysis of iNCs

To investigate iNC survival and functional integration in vivo, we transplanted the iNCs into the corpus callosum of severe combined immunodeficiency mice. One week postinduction, shp53 GFP-iNCs were injected into the right side of the corpus callosum of mice (the left side as nontransplanted controls). Grafted mice were euthanized, and their brains were sectioned 1 week, 2 weeks, and 4 months after transplantation. Immunohistochemistry revealed that the donor GFP-iNCs were restricted to the injection site within the cortex 1 week after transplantation (Figure 3D). MAP2- and Synapsin-positive iNCs were detected 2 weeks after transplantation (Figure 3E), suggesting the iNCs can be converted into mature neurons in vivo. Only ~20% of the grafted cells survived and showed MAP2- and Synapsin-positive staining 2 weeks after transplantation (n = 6; mouse number). For 4 months after transplantation of shp53-iNCs in mice (n = 6), we did not observe tumor formation, indicating that postmitotic iNCs did not possess oncogenicity in vivo.

p53 Regulates a Set of Defined Transcription Factors in iN Conversion

What is the mechanism underlying shp53-induced fibroblast-neuron conversion? We addressed this question by examining mRNA levels of many factors reported to be involved

in fibroblast-neuron conversion (Caiazzo et al., 2011; Vierbuchen et al., 2010; Pfisterer et al., 2011; Pang et al., 2011; Yoo et al., 2011; Ambasudhan et al., 2011; Yang et al., 2011; Son et al., 2011; Ring et al., 2012). We found that, in iNCs induced by p53 knockout, three neurogenic transcription factors, Ascl1, Brn2, and Neurod2, were increased by >10-fold (Figures 4A and S4A), suggesting that these factors may be involved in fibroblast-neuron conversion induced by p53 depletion.

Expression of neurogenic transcription factors Ascl1, Brn2, Neurod2, or all three together in wild-type IMR90 cells could not induce fibroblast-neuron conversion (Figure S4B; see also Vierbuchen et al., 2010, Yoo et al., 2011, and Pang et al., 2011), suggesting that depletion of p53 does not induce neuron conversion solely by upregulation of these factors. However, expression of *Ascl1*, *Brn2*, or *Neurod2* together with *p53* knockdown or knockout in IMR90 cells significantly increased the rate of iNC induction as compared to p53 knockdown or knockout alone (Figure 4B). In these combinations, expression of Neurod2 with p53 depletion reached the highest efficiency of converting fibroblast to neurons. It should be pointed out that, for these experiments, we measured the conversion efficiency at 10 days after induction, when neuron conversion was increasing, but not reaching the plateau level. If we measured at 28 days after induction, at which p53 depletion converted most fibroblast to neurons (Figure 2F), expression of these three neurogenic transcription factors did not further increase the efficiency of neuron conversion (not shown). These results suggest that Ascl1, Brn2, and particularly Neurod2 may enhance the rate of p53-depletion-induced neuron conversion.

The present work described a mechanism that converts fibroblast to neurons with high efficiency, even within 3–10 days after neuron induction. Recent studies showed that various sets of transcription factors, such as Ascl1/Brn2/Mytl1 or miR9-124+Ascl1/Neurod2/Mytl1 could also induce fibroblast-neuron conversion (Yoo et al., 2011; Pang et al., 2011). Consistently, expression of these two sets of transcription factors in IMR90 cells induced neuron conversion in IMR90 cells (Figures 4C and S4C). However, the conversion efficiency, reflected in the kinetics of conversion and the ultimate percentage of fibroblast-neuron conversion, was lower than p53 knockdown alone (Figure 4C). When we repeated similar experiments in late-stage IMR90 cells (population doublings 55), expression of *Ascl1/Brn2/Mytl1* could barely induce any fibroblast-neuron conversion (~2% in 4 weeks), whereas shp53 or shp53+*Neurod2* induced conversion at a much-higher efficiency of ~10%–15% ($p < 0.01$; Figures 4D and S4D). The efficiency of conversion was in general much lower than that observed in early-stage IMR90 cells, likely because the expression of p53 is progressively upregulated in late-passage cells (Figure S4E; Deng et al., 2008; Yang, 2008). Thus, for late-stage IMR90 cells, the published method using a defined set of transcription factors nearly failed in inducing fibroblast-neuron conversion, whereas our method was much more successful in inducing fibroblast-neuron conversion.

p53 Binds to the Promoter DNA of Neurod2 to Regulate Fibroblast-Neuron Conversion

To address if depletion of p53 is specifically linked to the induction of neurogenic transcription factors, we performed quantitative chromatin immunoprecipitation assays. To determine if p53 binds to the promoter of these genes, we scanned the *Ascl1*, *Brn2*, and

Neurod2 promoters for potential p53-binding sites. There are at least three potential binding sequences in the Neurod2 promoter. PCR primers of *Neurod2* were designed to flank these sites, and primers of *Ascl1*, *Brn2*, and *p21* promoters were designed or used as previously described (Sachdeva et al., 2009; Kaeser and Iggo, 2002). The binding was assessed by the enrichment of real-time PCR signal in the anti-p53 sample compared to the no-antibody and control immunoglobulin G reactions. At IMR90 cells, p53 consistently bound to the *Neurod2* promoter region, which flanked one of the p53 consensus sites at chr17, 37763017-37763037 (Figure S4F). This binding was not observed in $p53^{-/-}$ cells. The weak binding signal was observed in the other two binding sites of Neurod2 (data not shown). PCR amplifications of *Ascl1* and *Brn2* promoter regions failed to show enrichment in binding signal (Figure S4F). As a positive control, p53 bound to *p21* promoter. Furthermore, we treated SH-SY5Y (a human neuroblastoma cell line with wild-type p53) with doxorubicin, which caused upregulation of the endogenous p53 (data not shown). From the same treated cells, we detected a 3-fold decrease in the *Neurod2* mRNA level as compared with no drug treatment (Figure S4G). This was accompanied by a 3- to 4-fold increase in p53 binding to *Neurod2* and *p21* promoters (Figure S4H). These results indicate that p53 binds to the Neurod2 promoter in cells.

To further investigate the functional relationship between p53 and Neurod2, we examined their effects on fibroblast-neuron conversion. IMR90 cells coexpressing shp53 and sh-Neurod2 were cultured in neuronal induction medium. Knockdown of *Neurod2* decreased the rate of fibroblast-neuron conversion in IMR90 cells expressing shp53 (Figure S4I), demonstrating that p53-mediated fibroblast-neuron conversion requires Neurod2. Together with the data that p53 binds to the *Neurod2* promoter, we conclude that direct regulation of *Neurod2* transcription by p53 plays a role in p53-deficiency-dependent fibroblast-neuron conversion. However, depletion of *Neurod2* only partly blocked neuronal conversion of fibroblasts, indicating that p53 deficiency induces cell fate transformations on multiple targets. Depletion of *Ascl1* and *Brn2* did not affect p53-mediated fibroblast-neuron conversion, suggesting that p53 may indirectly regulate these genes during fibroblast-neuron conversion. Because we do not have evidence of interaction of p53 with Ascl1 and Brn2, the upregulations of these genes by depletion of p53 might be a consequence of the conversion process.

Genome-wide Transcriptional Profiling of Induced Neurons

To analyze the similarities between iNCs and parental fibroblasts, we generated comparative global gene expression data by microarray analysis. Microarray data were quantile normalized and filtered based on the average signal, and differently expressed genes were selected for further analysis. Hierarchical cluster analysis revealed a significant difference between shp53-iNCs and their parental IMR90 cells (Figures 4E and 4F). Although there are subtle differences in the global gene expression profiles of the iNCs tested (shp53 day 7 and day 21), all of them are clearly distinct from both parental IMR90 and shp53 IMR90 fibroblasts. The clustering analysis of global gene expression revealed that iNCs by miR9-124+Ascl1/Neurod2/Mytl1 are particularly similar to the shp53 iNCs (Figures 4E and 4F), indicating that iNCs generated by different methods show similarity of gene expression profiling. By analysis of the 4-folds-changed genes of the microarray data, all iNCs showed

the general degree of gene expression overlap. For gene-enrichment analysis, we found that particular markers of different germ layers were significantly changed in shp53 fibroblasts and iNCs compared with those in parental fibroblasts. We also analyzed expressions of fibroblast-specific genes during neuronal conversion. Expressions of 59 and 68 fibroblast-specific genes were significantly changed in iNCs (day 7 and day 21) relative to wild-type IMR90, respectively, and 42 genes from the two groups (day 7 and day 21) were the same (71.2% and 61.8%, respectively). These data suggest that there may be permanent downregulation of a set of fibroblast-specific genes during neuronal conversion. Taken together, these findings indicate that the genetic transdifferentiation erased the majority of the evident expression hallmarks of the cell of origin whereas specifically inducing the neuronal phenotype.

Collectively, our data showed that inhibition of p53 efficiently induces conversion of fibroblasts to neurons. This finding may have widespread impact in our understanding and development of neuron-replacement therapy. We provided a method for converting most fibroblasts to neurons within only 1 week of time. Moreover, the defined transcription factors failed in inducing fibroblast-neuron conversion in late-passage fibroblasts. Our method of depleting p53 is advantageous in inducing neuron in both early- and late-passage fibroblast cells. The present work may improve the understanding of the mechanisms involved in cell differentiation and reprogramming, particularly about the role of p53. Direct lineage conversions between very distantly related cell types might involve two main steps: (1) reprogramming of prior donor cells into induced progenitors, which might not pass through a pluripotent state, and (2) subsequent redifferentiation into a complete and functional lineage. Our finding that depletion of p53 causes conversion of fibroblast to neurons suggests that p53 may inhibit both steps. We found that depletion of p53 alone could induce iNCs, but its efficiency was increased as we comanipulated other transcription factors, like Neurod2. These combinations could rapidly generate neural progenitors (70% iNCs within 1 week), which will provide a powerful approach for the clinical utility. Furthermore, these results also suggest that p53 may act as a “master regulator” to coordinate a set of defined factors in blocking cell reprogramming in physiological conditions.

There is a clear limitation of generating induced mature neurons in vitro for cell-based clinical application (Yang et al., 2011). Because such therapies need large numbers of iNCs, induced mature neurons are terminally differentiated neurons that are unable to expand. Alternatively, neural progenitors or immature neural cells prepared in vitro might generate different neural lineages in vivo including mature neurons (Kim et al., 2011). Our results indicate that p53 deficiency induces three neural lineages and coculture of iNCs with primary neurons could enhance neuron maturation, suggesting that targeting the p53 pathway to generate functional neural tissues in vivo might be especially important.

EXPERIMENTAL PROCEDURES

Neural Cell Conversion

For neuronal conversion, modified fibroblasts were plated in Dulbecco's modified Eagle's medium at a density of 3.0×10^4 cells per cm^2 on microscope glass coverslips coated with

Matrigel (BD Biosciences) or laminin (Roche) and fibronectin (Sigma-Aldrich) in 35 mm dish. Four days after infection, the media was changed to neuronal media (ScienCell; no. 1521) plus 0.5 mM dibutyryl cyclic AMP sodium salt (Sigma-Aldrich) and 20 ng ml^{-1} basic fibroblast growth factor (ScienCell). We also added 10 ng ml^{-1} human brain-derived neurotrophic factor and neurotrophin-3 (both from PROSPEC) after 2 weeks to the medium to enhance induced cell survival. For astrocyte induction, we used astrocyte medium from ScienCell (no. 1801). We calculated the induction efficiencies using the numbers of the induction efficiencies representing the percentage of induced neural cells at the time point of quantification (n = 1,000; 20 random visual fields/three wells for each sample). Quantitation of percent iNCs is counted by Tuj1 (early stage, before 1 week induction) and MAP2 (late stage, after 1 week induction)-positive staining, astrocytes by GFAP, and oligodendrocytes by O4-positive staining. Quantitative data are mean ± SEM from five biologically independent experiments. Animal experiments were approved by the Institutional Animal Care and Use Committees of the Washington University in St. Louis.

Supplementary Material

Refer to Web version on PubMed Central for supplementary material.

ACKNOWLEDGMENTS

We thank Andrew Yoo for helpful suggestions and reagents and Buck Rogers and Wilbur Song for proofreading this manuscript. We thank the Genome Technology Access Center in the Department of Genetics at Washington University School of Medicine for help with genomic analysis. This work is supported in part by grants from the Natural Science Foundation (no. 81228017), the Science and Technology Support Program (no. 2014SK3243), and Ministry of Science and Technology (863 program 2011AA020113).

REFERENCES

Abbas T, Dutta A. p21 in cancer: intricate networks and multiple activities. Nat. Rev. Cancer. 2009; 9:400–414. [PubMed: 19440234]

Ambasudhan R, Talantova M, Coleman R, Yuan X, Zhu S, Lipton SA, Ding S. Direct reprogramming of adult human fibroblasts to functional neurons under defined conditions. Cell Stem Cell. 2011; 9:113–118. [PubMed: 21802386]

Caiazzo M, Dell'Anno MT, Dvoretskova E, Lazarevic D, Taverna S, Leo D, Sotnikova TD, Menegon A, Roncaglia P, Colciago G, et al. Direct generation of functional dopaminergic neurons from mouse and human fibroblasts. Nature. 2011; 476:224–227. [PubMed: 21725324]

Deng Y, Chan SS, Chang S. Telomere dysfunction and tumour suppression: the senescence connection. Nat. Rev. Cancer. 2008; 8:450–458. [PubMed: 18500246]

Goh AM, Coffill CR, Lane DP. The role of mutant p53 in human cancer. J. Pathol. 2011; 223:116–126. [PubMed: 21125670]

Hede SM, Nazarenko I, Nistér M, Lindström MS. Novel Perspectives on p53 Function in Neural Stem Cells and Brain Tumors. J. Oncol. 2011; 2011:852970. [PubMed: 21209724]

Hofseth LJ, Robles AI, Yang Q, Wang XW, Hussain SP, Harris C. p53: at the crossroads of molecular carcinogenesis and molecular epidemiology. Chest Suppl. 2004; 125:83S–85S.

Hong H, Takahashi K, Ichisaka T, Aoi T, Kanagawa O, Nakagawa M, Okita K, Yamanaka S. Suppression of induced pluripotent stem cell generation by the p53-p21 pathway. Nature. 2009; 460:1132–1135. [PubMed: 19668191]

Kaeser MD, Iggo RD. Chromatin immunoprecipitation analysis fails to support the latency model for regulation of p53 DNA binding activity in vivo. Proc. Natl. Acad. Sci. USA. 2002; 99:95–100. [PubMed: 11756653]

Kawamura T, Suzuki J, Wang YV, Menendez S, Morera LB, Raya A, Wahl GM, Izpisúa Belmonte JC. Linking the p53 tumour suppressor pathway to somatic cell reprogramming. Nature. 2009; 460:1140–1144. [PubMed: 19668186]

Kim J, Efe JA, Zhu S, Talantova M, Yuan X, Wang S, Lipton SA, Zhang K, Ding S. Direct reprogramming of mouse fibroblasts to neural progenitors. Proc. Natl. Acad. Sci. USA. 2011; 108:7838–7843. [PubMed: 21521790]

Laiho M, Latonen L. Cell cycle control, DNA damage checkpoints and cancer. Ann. Med. 2003; 35:391–397. [PubMed: 14572162]

Lanni C, Racchi M, Memo M, Govoni S, Uberti D. p53 at the crossroads between cancer and neurodegeneration. Free Radic. Biol. Med. 2012; 52:1727–1733. [PubMed: 22387179]

Mendrysa SM, Ghassemifar S, Malek R. p53 in the CNS: Perspectives on Development, Stem Cells, and Cancer. Genes Cancer. 2011; 2:431–442. [PubMed: 21779511]

Pang ZP, Yang N, Vierbuchen T, Ostermeier A, Fuentes DR, Yang TQ, Citri A, Sebastiano V, Marro S, Südhof TC, Wernig M. Induction of human neuronal cells by defined transcription factors. Nature. 2011; 476:220–223. [PubMed: 21617644]

Pfisterer U, Kirkeby A, Torper O, Wood J, Nelander J, Dufour A, Björklund A, Lindvall O, Jakobsson J, Parmar M. Direct conversion of human fibroblasts to dopaminergic neurons. Proc. Natl. Acad. Sci. USA. 2011; 108:10343–10348. [PubMed: 21646515]

Ring KL, Tong LM, Balestra ME, Javier R, Andrews-Zwilling Y, Li G, Walker D, Zhang WR, Kreitzer AC, Huang Y. Direct reprogramming of mouse and human fibroblasts into multipotent neural stem cells with a single factor. Cell Stem Cell. 2012; 11:100–109. [PubMed: 22683203]

Sachdeva M, Zhu S, Wu F, Wu H, Walia V, Kumar S, Elble R, Watabe K, Mo YY. p53 represses c-Myc through induction of the tumor suppressor miR-145. Proc. Natl. Acad. Sci. USA. 2009; 106:3207–3212. [PubMed: 19202062]

Son EY, Ichida JK, Wainger BJ, Toma JS, Rafuse VF, Woolf CJ, Eggan K. Conversion of mouse and human fibroblasts into functional spinal motor neurons. Cell Stem Cell. 2011; 9:205–218. [PubMed: 21852222]

Takahashi K, Tanabe K, Ohnuki M, Narita M, Ichisaka T, Tomoda K, Yamanaka S. Induction of pluripotent stem cells from adult human fibroblasts by defined factors. Cell. 2007; 131:861–872. [PubMed: 18035408]

Thier M, Wörsdörfer P, Lakes YB, Gorris R, Herms S, Opitz T, Seiferling D, Quandel T, Hoffmann P, Nöthen MM, et al. Direct conversion of fibroblasts into stably expandable neural stem cells. Cell Stem Cell. 2012; 10:473–479. [PubMed: 22445518]

Utikal J, Polo JM, Stadtfeld M, Maherali N, Kulalert W, Walsh RM, Khalil A, Rheinwald JG, Hochedlinger K. Immortalization eliminates a roadblock during cellular reprogramming into iPS cells. Nature. 2009; 460:1145–1148. [PubMed: 19668190]

Vierbuchen T, Ostermeier A, Pang ZP, Kokubu Y, Südhof TC, Wernig M. Direct conversion of fibroblasts to functional neurons by defined factors. Nature. 2010; 463:1035–1041. [PubMed: 20107439]

Yang Q. Cellular senescence, telomere recombination and maintenance. Cytogenet. Genome Res. 2008; 122:211–218. [PubMed: 19188689]

Yang Q, Zhang R, Wang XW, Spillare EA, Linke SP, Subramanian D, Griffith JD, Li JL, Hickson ID, Shen JC, et al. The processing of Holliday junctions by BLM and WRN helicases is regulated by p53. J. Biol. Chem. 2002; 277:31980–31987. [PubMed: 12080066]

Yang Q, Zhang R, Wang XW, Linke SP, Sengupta S, Hickson ID, Pedrazzi G, Perrera C, Stagljar I, Littman SJ, et al. The mismatch DNA repair heterodimer, hMSH2/6, regulates BLM helicase. Oncogene. 2004; 23:3749–3756. [PubMed: 15064730]

Yang N, Ng YH, Pang ZP, Südhof TC, Wernig M. Induced neuronal cells: how to make and define a neuron. Cell Stem Cell. 2011; 9:517–525. [PubMed: 22136927]

Yoo AS, Sun AX, Li L, Shcheglovitov A, Portmann T, Li Y, Lee-Messer C, Dolmetsch RE, Tsien RW, Crabtree GR. MicroRNA-mediated conversion of human fibroblasts to neurons. Nature. 2011; 476:228–231. [PubMed: 21753754]

Highlights

- Depletion of *p53* alone converts fibroblasts into three major neural lineages
- The induced neurons are functional in vitro and in vivo
- *p53* regulates neurogenic transcription factors for fibroblast-neuron conversion
- Genome-wide transcription profile is altered during fibroblast-neuron conversion

In Brief

Conversion from fibroblast to neuron has recently been successfully induced. However, the underlying mechanisms are poorly understood. Zhou et al. found that depletion of *p53* alone converted fibroblasts into three major neural lineages. This finding may help understanding reprogram mechanisms and developing cell-based replacement therapies to neurological disorders.

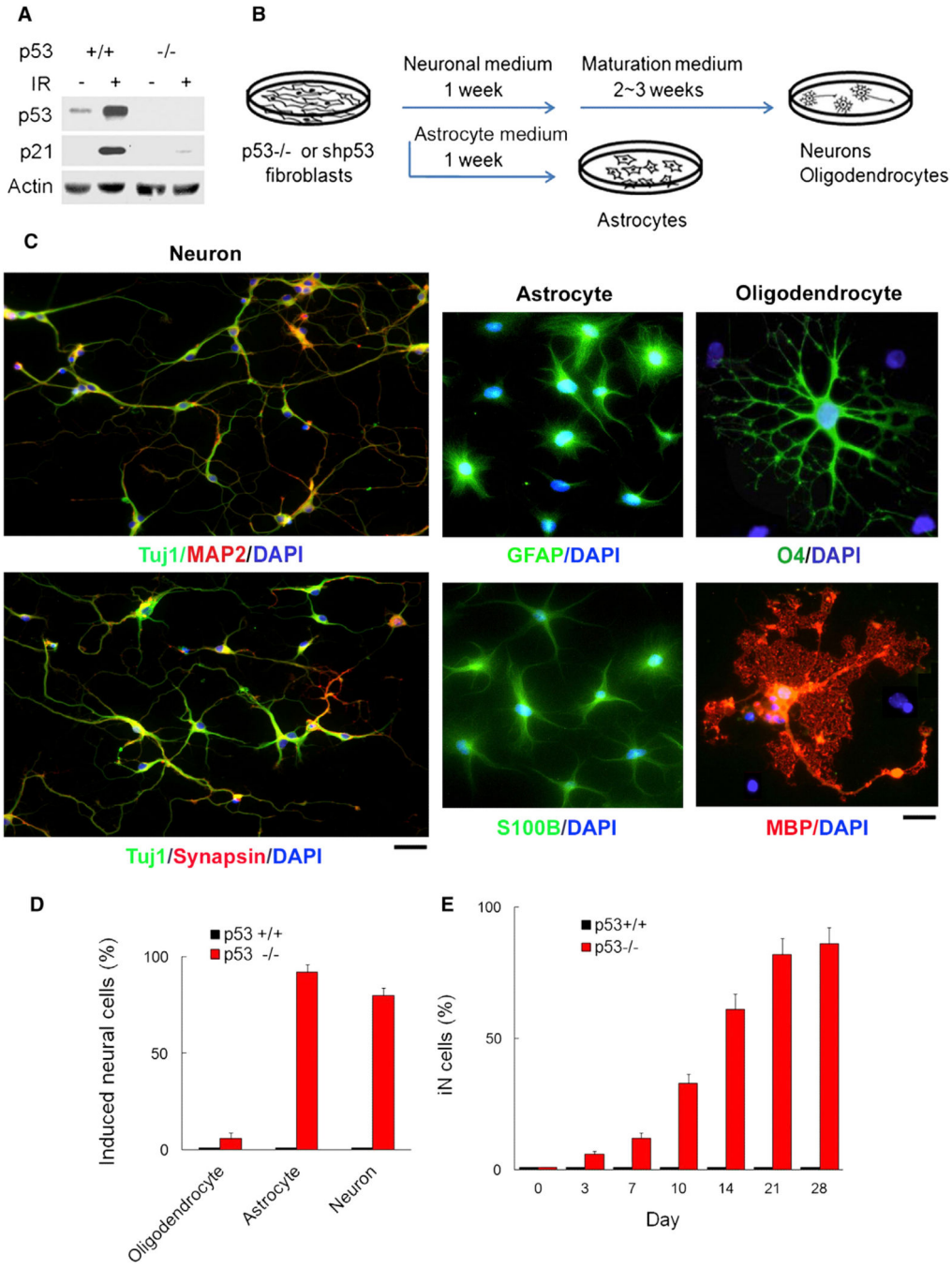

Figure 1. Conversion of Human Fibroblasts into Neural Cells by Knockout of *p53*

(A) Knockout of *p53* by ZFNs in normal human primary fibroblasts IMR90. p53 protein expression is erased, and p21 protein is markedly decreased in *p53* knockout cells by ZFNs. Expression of p53 and p21 in parental IMR90 cells (+/+) and IMR90 cells with targeted deletion of both *p53* alleles (−/−) before and 24 hr after 5 Gy radiation (IR) assessed by western blot analysis.

(B) Schematic drawing of the experimental strategy to derive induced neural cells.

(C) Characterization of neural cells derived from *p53*$^{-/-}$ IMR90 cells. The images show the induced O4- and MBP-positive oligodendrocytes, GFAP- and S100B-positive astrocytes, and Tuj1/MAP2, Synapsin-positive neurons. The scale bar represents 10 μm.
(D) Quantification of induced oligodendrocytes (3 weeks after induction; $p < 0.01$), neurons (3 weeks; $p < 0.001$), and astrocytes (2 weeks; $p < 0.001$) from *p53*$^{+/+}$ and *p53*$^{-/-}$ IMR90 cells. The induction efficiencies were calculated using the numbers of the induction efficiencies representing the percentage of induced neural cells at the time point of quantification (n = 1,000; counted cell number). Quantitation of percent iNCs is counted by MAP2-positive staining, astrocytes by GFAP, and oligodendrocytes by O4-positive staining.
(E) Kinetic analysis of iNCs from *p53*$^{+/+}$ and *p53*$^{-/-}$ IMR90 cells after induction. Quantitation of percent iNCs is counted by Tuj1 (early stage, before 1 week)- and MAP2 (late stage, after 1 week)-positive staining (counted cell number: n = 1,000). Quantitative data are mean ± SEM from five biologically independent experiments. The p values are <0.001 between control and treatment groups, based on Student's t test.
See also Figure S1.

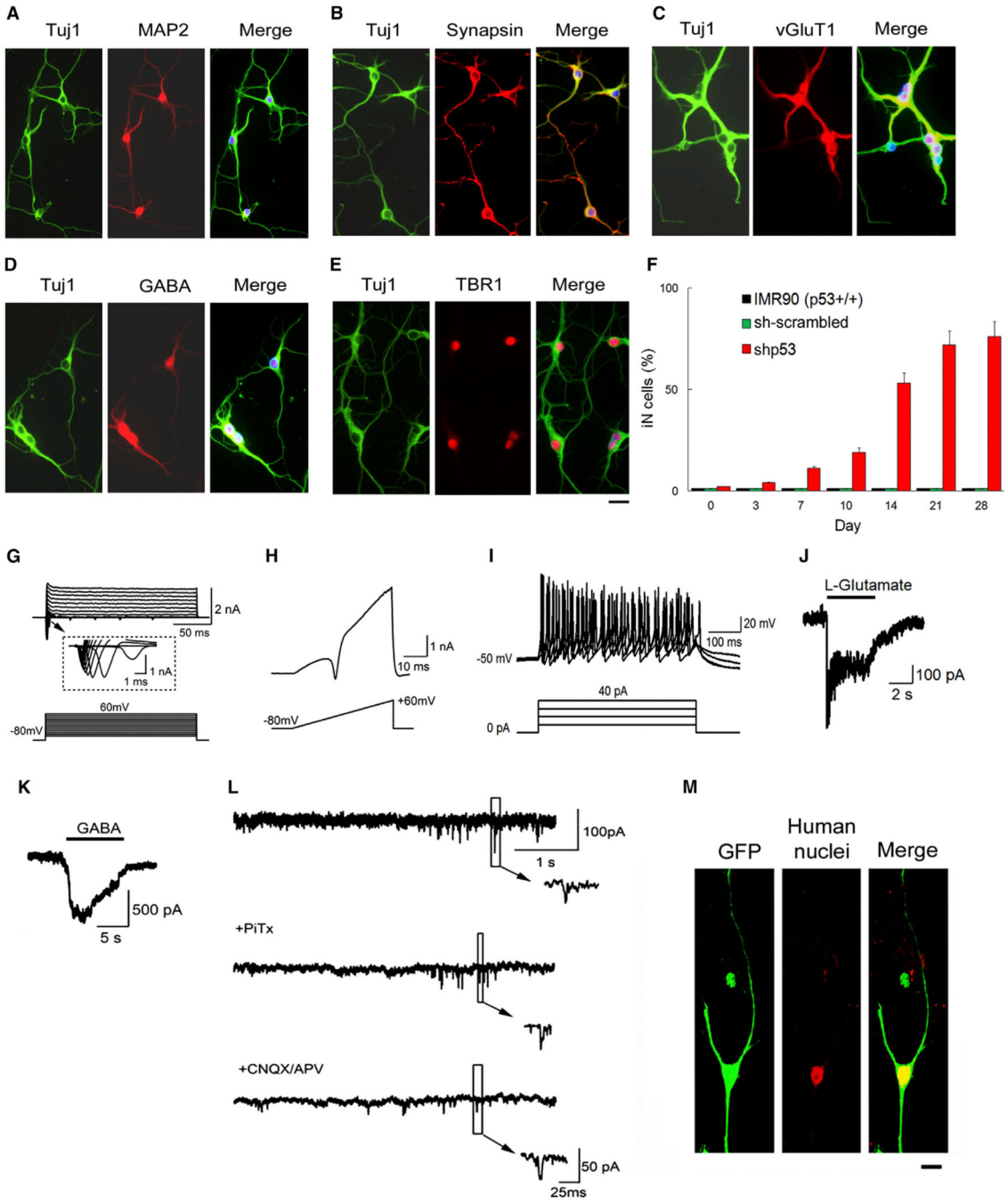

Figure 2. *p53* shRNAs Convert Human Fibroblasts into Functional Neurons

(A–E) Expression of Tuj1, MAP2, Synapsin, vGluT1, GABA, and TBR1 in iNCs from shp53 IMR90 fibroblasts 3 weeks after induction. The scale bar represents 10 μm.

(F) Kinetic analysis of iNCs from IMR90 cells with or without expressing shp53 or scrambled shRNA (counted cell number: n = 1,000). The p values are <0.001 between control and treatment groups, based on Student's t test. Quantitative data are mean ± SEM from five biologically independent experiments.

(G–L) Electrophysiological characterization of shp53 iNCs. (G) Representative current traces (upper panel) recorded in voltage-clamp mode. Cells were depolarized by voltage steps from −60 to +60 mV in 10 mV increments (Δ10 mV, upper panel). The lower panel shows the current-voltage (I-V) relationship for sodium current. (H) Representative traces of membrane currents recorded with a ramp protocol (lower panel, a voltage ramp from −80 mV to +60 mV over 500 ms). Fast-activating Na^+ currents were prominent. (I) Traces of evoked action potential in current-clamp mode. Step currents were injected from 0 pA to 60 pA in 10 pA increments. (J and K) Local application of either 15 mM L-glutamate (J) or 15 mM GABA (K) elicited current responses. (L) Sample traces of spontaneous synaptic currents (top; without pharmacological blockers), miniature EPSCs (mEPSCs) (middle; with 100 μM picrotoxin to block GABAA receptor), and miniature IPSCs (mIPSCs) (bottom; with 20 μM CNQX to block AMPA receptor and 50 μM AP-5 to block NMDA receptor) recorded at a holding potential of −80 mV. The presence of mEPSCs and mIPSCs indicates that iNCs are able to form functional neuronal connections.

(M) Positive staining of human nuclei (specific marker for human cells) in all GFP-labeled iNCs indicates that electrophysiological recordings are from iNCs. The scale bar represents 10 μm.

See also Figure S2.

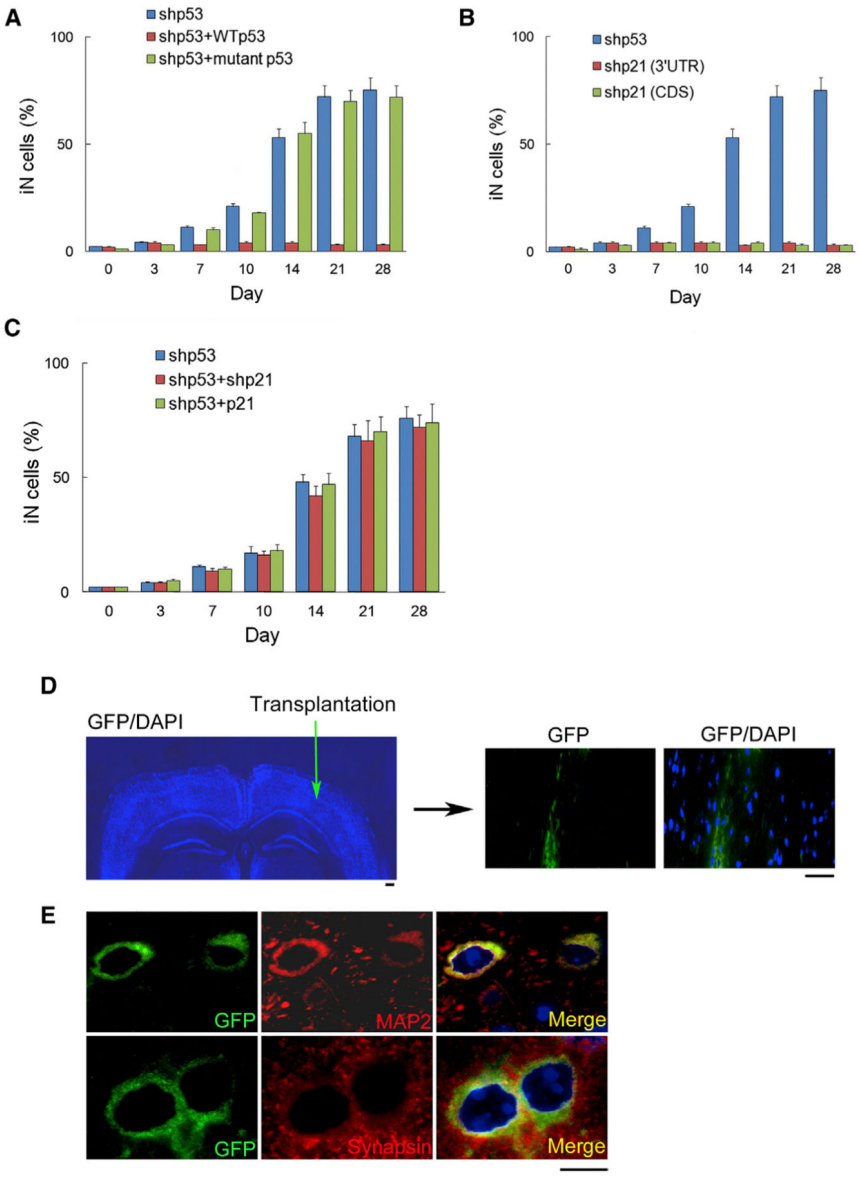

Figure 3. Effects of p53 and p21 on iNC Conversion

(A) Wild-type p53, but not mutant p53, blocks conversion of IMR90 cells into iNCs by shp53. Lentiviral wild-type or mutant (R273H) p53 was expressed in IMR90 cells with expression of shp53 (targeting 3′ UTR). After induction in the indicated time points, iNCs were identified by morphology and Tuj1-positive staining. Quantitative data indicate iNCs from shp53, shp53+wild-type ($p < 0.001$ on days 7–28), or mutant p53 cells ($p > 0.5$ on days 7–28).

(B and C) Quantitative data of iNCs from IMR90 cells with expressions of shp53 and shp21 (B; $p < 0.001$ on days 7–28) or from IMR90 cells with expressions of shp53, shp53+shp21, or shp53+wild-type p21 (C; $p > 0.5$). Quantitative data are mean ± SEM from five biologically independent experiments (counted cell number per sample: n = 1,000). The p values are based on Student's t test.

(D and E) Transplantation of shp53-iNCs in mice. (D) Schematic representation of iNC transplantation and grafted GFP+ cells in the brain cortex 1 week after transplantation. The scale bar represents 50 μm. (E) iNCs express the mature neuronal markers MAP2 and Synapsin 2 weeks after transplantation. The scale bar represents 10 μm.
See also Figure S3.

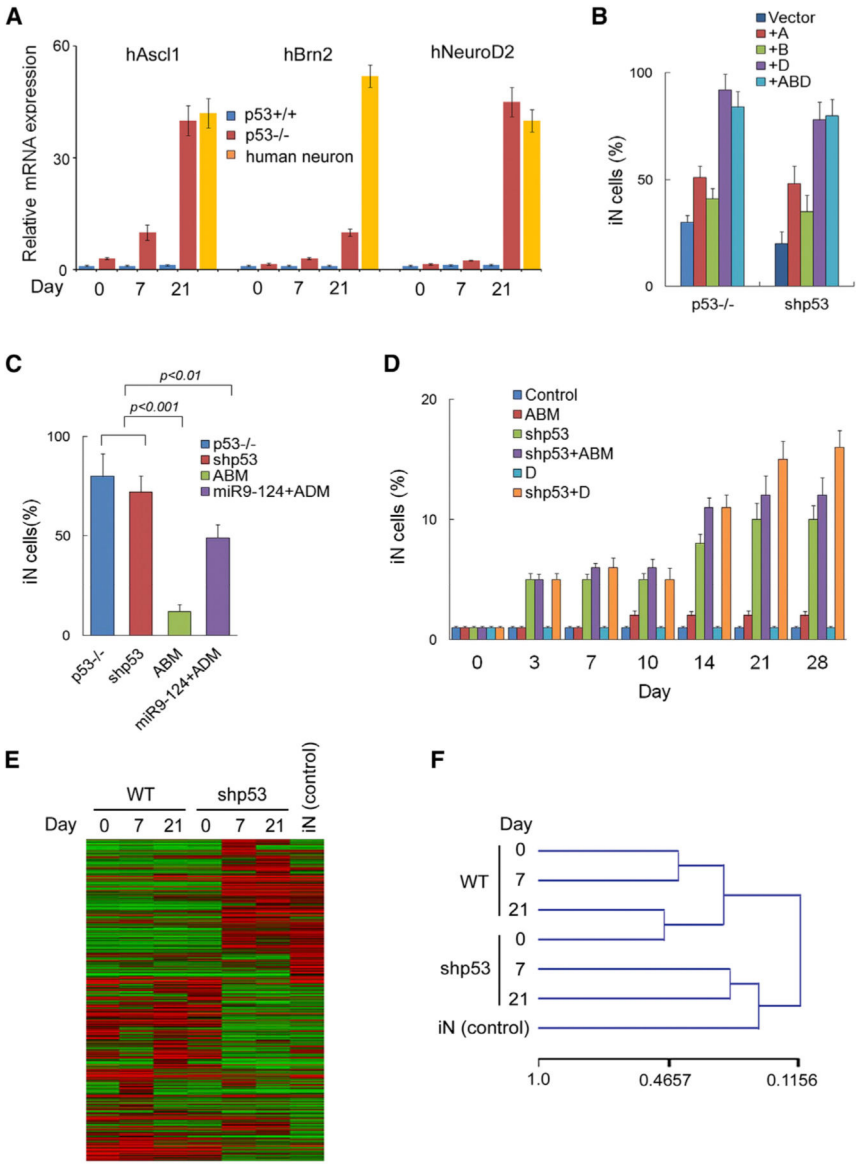

Figure 4. Combinational Effects of p53 with Defined Transcription Factors during Conversion

(A) qRT-PCR results show mRNA level of defined transcription factors in IMR90 control, $p53^{-/-}$, $p53^{-/-}$ iNCs, and human primary neurons (n = 3 experiments).

(B) Quantitative data represent the percentage of iNCs from $p53^{-/-}$ and shp53 IMR90 cells with coexpression indicating defined factors 10 days after induction. A, Ascl1; B, Brn2; D, Neurod2 (count cell number: n = 1,000). The p values are <0.001 between vector and +D or ABD, based on Student's t test.

(C) Comparison of iNC-converting efficiency among $p53^{-/-}$, shp53, ABM (M, Myt1l), and miR-9-124+ADM 3 weeks after induction from IMR90 cells. The graph represents the percentage of iNCs. The p values are based on Student's t test.

(D) Quantitative data represent iNCs from indicated defined factors after induction in late-stage IMR90 cells (PD55; count cell number: n = 1,000).

(A–D) Quantitative data are mean ± SEM from three biologically independent experiments.

(E and F) Global gene-expression profiling of iNCs. (E) Heatmap of genes differentially expressed in global RNA-microarray analysis performed on IMR90s (wild-type [WT]), shp53 IMR90 fibroblasts, shp53 iNCs (day 7 and day 21), and positive control iNCs (miR-9-124+Ascl1/Myt1l/Neurod2). (F) Hierarchical clustering.
See also Figure S4.